

1 Vector dynamics influence spatially imperfect genetic
2 interventions against disease

3 Mete K Yuksel

4 Department of Mathematics, University of Idaho, Moscow, ID
5 83844-1103 USA
6 yuks1141@vandals.uidaho.edu

7
8 Christopher H Remien

9 Department of Mathematics, University of Idaho, Moscow, ID
10 83844-1103 USA
11 cremien@uidaho.edu

12
13 Bandita Karki

14 Department of Mathematics, University of Idaho, Moscow, ID
15 83844-1103 USA
16 kark6289@vandals.uidaho.edu

17
18 James J Bull

19 Department of Biological Sciences, University of Idaho, Moscow, ID
20 83844-1103 USA
21 jbull@uidaho.edu

22
23 Stephen M Krone*

24 Department of Mathematics, University of Idaho, Moscow, ID
25 83844-1103 USA
26 krone@uidaho.edu

27 *Corresponding author

28

July 16, 2020

29

Abstract

30

Background and objectives: Genetic engineering and similar technologies offer promising new approaches to controlling human diseases by blocking transmission from vectors. However, in spatially structured populations, imperfect coverage of the vector will leave pockets in which the parasite can persist. Yet movement by humans may disrupt this local persistence and facilitate eradication when these pockets are small, essentially distributing parasite reproduction out of unprotected areas and into areas that block its reproduction.

31

Methodology: We develop formal mathematical models of this process similar to standard Ross-Macdonald models, but (i) specifying spatial structure of two patches, with transmission blocked in one patch but not in the other, (ii) allowing temporary human movement (travel instead of migration), and (iii) considering two different modes of mosquito biting.

32

Results: We find that there is no invariant effect of disrupting spatial structure with travel. For both biting models, travel out of the unprotected patch has different consequences than travel by visitors into the patch, but the effects are reversed between the two biting models.

33

Conclusions and implications: Overall, the effect of human travel on the maintenance of vector-borne diseases in structured habitats must be considered in light of the actual biology of mosquito abundances and biting dynamics.

34

Lay summary: Genetic interventions against pathogens transmitted by insect vectors are promising methods of controlling infectious diseases. These interventions may be imperfect, leaving pockets where the parasite persists. How will human movement between protected and unprotected areas affect persistence? Mathematical models developed here show that the answer is ecology-dependent, depending on vector biting behavior.

35

36

37

38

39

40

41

42

43

44

45

46

47

48

49

50

51

52

53

54

55

56

Keywords: genetic pest management, gene drive, pathogen suppression, mosquito biting dynamics, spatial structure, Ross-Macdonald, mathematical model

57

Introduction

58

59

60

61

62

63

64

65

66

67

68

69

70

71

72

73

74

75

76

77

78

79

80

81

82

83

84

85

86

87

88

89

90

91

92

93

94

95

96

97

98

99

100

101

102

103

104

105

106

107

108

109

110

111

112

113

114

115

116

117

118

119

120

121

122

123

124

125

126

127

128

129

130

131

132

133

134

135

136

137

138

139

140

141

142

143

144

145

146

147

148

149

150

151

152

153

154

155

156

157

158

159

160

161

162

163

164

165

166

167

168

169

170

171

172

173

174

175

176

177

178

179

180

181

182

183

184

185

186

187

188

189

190

191

192

193

194

195

196

197

198

199

200

201

202

203

204

205

206

207

208

209

210

211

212

213

214

215

216

217

218

219

220

221

222

223

224

225

226

227

228

229

230

231

232

233

234

235

236

237

238

239

240

241

242

243

244

245

246

247

248

249

250

251

252

253

254

255

256

257

258

259

260

261

262

263

264

265

266

267

268

269

270

271

272

273

274

275

276

277

278

279

280

281

282

283

284

285

286

287

288

289

290

291

292

293

294

295

296

297

298

299

300

301

302

303

304

305

306

307

308

309

310

311

63 parallel approach, but without genetic engineering, introduces pathogen-blocking strains
64 of the self-spreading bacterial symbiont *Wolbachia* into the vector (Hoffmann et al.,
65 2011; Schmidt et al., 2017). A third, and more mundane approach is to release huge
66 numbers of lab-reared, genetically modified vectors, simply to infuse wild populations
67 with transmission-blocking genes in a manner akin to the sterile insect technique (Evans
68 et al., 2019; Gould et al., 2006). The gene drive and *Wolbachia* approaches result in
69 possibly permanent alterations of vector populations because the genetic modifications
70 are selectively maintained. The swamping method is typically transient, because the
71 modification is not coupled with any selective benefit (Gould et al., 2006); continual
72 releases of engineered vectors would be required to maintain the parasite block.

73 Genetic modifications have an advantage in that they accrue directly and
74 specifically to the vector and are transmitted intact to offspring, contrasting with
75 pesticides that are broadcast environmentally, cannot be uniformly applied and need to
76 be applied repeatedly. However, genetic methods are sometimes controversial and face
77 extreme regulatory hurdles because of their transgenerational permanence. We
78 nonetheless imagine that many of these genetic technologies will be widely implemented
79 in the near future, so predicting the possible bases of failure versus success may be
80 useful in ensuring the best possible outcomes. Some methods may seem so foolproof as
81 to ensure disease eradication because of their ability to modify huge fractions of vector
82 populations. Even so, one worry is that any population intervention is likely to be
83 somewhat incomplete, leaving spatial pockets of minimal coverage interspersed with
84 perhaps large pockets of almost total coverage (e.g., North et al., 2013, 2019). What
85 will be the effect of these pockets of poor coverage? From a greatly simplified spatial
86 model of pathogen dynamics, we previously suggested that spatial structure will foster
87 the persistence of the pathogen when the pathogen would disappear in the absence of
88 structure (Bull et al., 2019). Thus, any softening of spatial structure would help limit
89 parasite persistence. That model omitted vectors as well as hosts, so any inference to
90 vector dynamics was tangential. Here we consider a more realistic model of spatial
91 structure than we addressed previously: a model that includes vectors, with host
92 mobility; when hosts are spatially clustered and a genetic intervention blocks vector
93 transmission most places, does host movement invariably facilitate eradication?
94 Furthermore, how does the effect of human movement depend on the transmission
95 dynamics?

96 Our question has many precedents in previous mathematical models of vectored
97 diseases, of which the Ross-Macdonald models are the original and most prominent
98 (Keeling and Rohani, 2008). The effect of spatial structure on disease dynamics has
99 been addressed in several modeling studies when assuming a single model of
100 transmission dynamics (Cosner et al., 2009; Prosper et al., 2012; Ruktanonchai et al.,

101 2016; Anzo-Hernández et al., 2019; Soriano-Paños et al., 2020; Khamis et al., 2020).
102 The effect of different models of transmission dynamics has been addressed in the
103 absence of spatial structure (McCallum et al., 2001; Wonham et al., 2006). Our models
104 will combine spatial structure, differential blocking of transmission among patches,
105 human movement among patches, and different forms of mosquito biting dynamics. Our
106 assemblage of assumptions is unique, but this broad foundation of previous work
107 simplifies our task and provides many anchor points to validate our findings.

108 Results

109 Foundations

110 The Introduction provided several biological contexts for the problem we study. They
111 all involve vectored infectious diseases, spatial structure, and movement of vectors
112 and/or humans (we consider only the latter here). Here we explain how that biology is
113 converted into our models.

114 Population structure

115 Our models are standard epidemiological ‘SIS’ models, accounting for vector (mosquito)
116 and host (human) numbers, as well as spatial structure. Parasites have no individual
117 existence *per se* in the model; they exist only as infected states of mosquitoes or
118 humans. Infections are transmitted only mosquito to human or human to mosquito. A
119 full description of the mathematical models is given in the Appendix.

120 To abstract this biological process, we model a population with discrete
121 subpopulations; the same population subdivisions coincide for both humans and
122 vectors, but it operates somewhat differently for humans than for vectors. The number
123 of humans in each patch is invariant; no one is born and no one dies during the time
124 period considered. In contrast, mosquitoes have a patch-specific birth rate (independent
125 of the number of mosquitoes and humans) and a patch-invariant death rate, leading to
126 a patch-specific equilibrium density; mosquito lifetimes, on the order of weeks or
127 months, are much shorter than human lifetimes. Mosquito spatial structure is rigid and
128 invariant, whereas humans have a home patch but travel temporarily to non-resident
129 locations—a movement scheme that differs from formal ‘migration’ (Cosner et al.,
130 2009). The state of mosquito infections at a location depends on mosquito behavior and
131 on the history of their exposure to humans at that location, regardless of whether the
132 humans were residents or visitors. In contrast, humans are not confined to one location
133 throughout life; they move, but each person is identified with a home residence,
134 regardless of their location at any moment. This process would arise with daily

135 commuting, jobs that involve travel, and even some kinds of nomadic lifestyles. (Our
136 approach thus differs from standard migration models in which individuals move
137 without memory of an individual's previous residence.) Because humans travel, their
138 infection status depends on their history of exposure to mosquitoes at the different
139 locations they have occupied.

140 **Transmission dynamics**

141 We consider two models of infection dynamics as they affect mosquito biting rates:
142 density-dependent and frequency-dependent (McCallum et al., 2001; Wonham et al.,
143 2006). These models differ in the way the biting rate of mosquitoes at a site scales with
144 the number of humans at that site (Fig. 1). In the density-dependent model,
145 characterized by a mass-action functional response, the rate at which a single person is
146 bitten is independent of the number of humans; in the frequency-dependent model,
147 characterized by a saturated functional response, the total number of bites is
148 determined by the number of mosquitoes, so adding more humans decreases the bite
149 rate per person unless mosquito density increases with human density. The standard
150 Ross-Macdonald models often assume frequency-dependence.

151 A fundamental difference between these models is easily grasped for spatial
152 structure in which human density differs among patches. In the density-dependent case,
153 if mosquito density is the same across patches, each human is bitten at the same rate
154 regardless of patch. In the frequency-dependent case, again for constant mosquito
155 densities, humans are bitten at a lower rate in the larger patch (i.e., the patch with
156 more humans); in the extreme, a parasite might be maintained only in the smaller
157 patch because the biting rate per person is too low in the large patch. Only by scaling
158 mosquito density with human density is it possible to maintain similar biting rates per
159 humans across patches of different sizes.

160 Other models of biting dynamics have been developed, such as hybrid models that
161 allow biting dynamics to vary across different host densities (Gandon, 2018; Xue et al.,
162 2018). These models usually build in density dependence at one extreme of human
163 density and frequency dependence at the other. Our use of models at both extremes
164 obviates the need for hybrid models, given that we can show a fundamental difference
165 between the two processes. The contrast of our models highlights the need to
166 understand mosquito dynamics before reaching any conclusions about the impact of
167 travel, and without an empirical basis for justifying even the hybrid models, hybrid
168 models cannot be justified biologically any more than can the extremes.

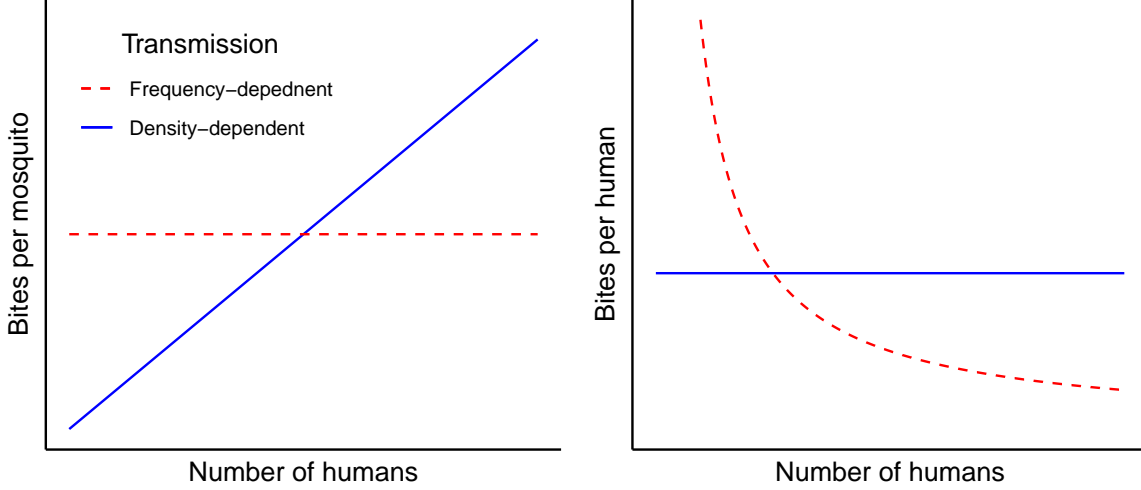


Figure 1: Differences between the frequency-dependent and density-dependent models with respect to biting dynamics. The left panel shows biting rate per mosquito, the right panel shows biting rate per human. The solid (blue) lines apply to the density-dependent case, dashed (red) to the frequency-dependent case.

¹⁶⁹ **\mathcal{R}_0 calculations when transmission is blocked in one patch**

¹⁷⁰ With vectored diseases, there are various ways to calculate the basic reproductive
¹⁷¹ number, \mathcal{R}_0 (e.g., Keeling and Rohani, 2008; Anzo-Hernández et al., 2019). Our
¹⁷² method (Appendix) is essentially that of Keeling and Rohani (2008). For our purposes,
¹⁷³ the actual value of \mathcal{R}_0 is unimportant, as we are interested in the relative impact on \mathcal{R}_0
¹⁷⁴ of changes in population structure, as well as a relative comparison of \mathcal{R}_0 for density
¹⁷⁵ dependence and frequency dependence. Typically, different methods of computing basic
¹⁷⁶ reproduction numbers in vector models can lead to different \mathcal{R}_0 values (e.g., one value
¹⁷⁷ being the square of what is obtained via a different method) but they agree at the
¹⁷⁸ epidemic threshold of $\mathcal{R}_0 = 1$, which again is the critical value between eradication and
¹⁷⁹ endemism.

¹⁸⁰ To keep the focus on biological relevance, we limit consideration to 2 patches. As
¹⁸¹ per our biological justification above, we let the intervention be fully effective and block
¹⁸² all transmission in patch 1, but absent in patch 2. Maintenance of the parasite ($\mathcal{R}_0 > 1$)
¹⁸³ in this setting is due entirely to whether the parasite persists in patch 2.

¹⁸⁴ We wish to consider conditions whereby, in the absence of human movement, the
¹⁸⁵ parasite would persist in patch 2. Our previous analysis (which neglected hosts and
¹⁸⁶ vectors, Bull et al., 2019) can be construed to suggest that, if patch 1 was sufficiently
¹⁸⁷ large, human movement between patches would facilitate parasite eradication by
¹⁸⁸ increasingly exposing the parasite to the average of both patches (as also true of
¹⁸⁹ Prosper et al. (2012)). We are interested in whether this conclusion holds: how does
¹⁹⁰ human movement affect persistence and how do the two models compare?

191 The \mathcal{R}_0 formula for either model (density-dependent or frequency-dependent) is a
 192 function of 7 parameters and 3 state variables (derived for general transmission values
 193 in the Appendix). The analysis assumes a small number of infected mosquitoes, an
 194 absence of infected humans in either patch, and no mosquito-to-human transmission in
 195 patch 1. For the frequency-dependent model with no mosquito-to-human transmission
 196 in patch 1, the formula is

$$\mathcal{R}_0^{\text{FD}} = \frac{\left[b_{FD}^2 \cdot a_{MH}^{(2)} \cdot a_{HM} \cdot M^{(2)} \right] \cdot \left[c_{22}^2 \cdot H^{(2)} + c_{12}^2 \cdot H^{(1)} \right]}{\gamma \cdot \delta \cdot \left[c_{22} \cdot H^{(2)} + c_{12} \cdot H^{(1)} \right]^2} \quad (\text{frequency dependent}), \quad (1)$$

197 with notation defined in Table 1. The first numerator term in brackets is a mosquito
 198 term that accounts for the number of mosquitoes, transmission rates per bite in both
 199 directions, and biting rates; the squared biting rate accounts for the mosquito
 200 acquisition of the parasite and then its later transmission. The second numerator term
 201 in brackets is one of human population size weighted by (squared) human travel
 202 probabilities to account for only those humans present in patch 2—the patch with no
 203 block to transmission. The denominator is a squared term of humans present in patch
 204 2, necessarily larger than the human term in the numerator given moderate or higher
 205 human densities (note that the $c_{ij} \leq 1$). Inspection of this result reveals how increasing
 206 the numbers of humans in patch 2, while holding the mosquito term constant, reduces
 207 $\mathcal{R}_0^{\text{FD}}$, reflecting the dilution of mosquito bites. These results have been confirmed with
 208 limited numerical analyses of the full equations by varying the c_{ij} . The threshold $\mathcal{R}_0 = 1$
 209 in (1) and (2) coincided with the threshold for maintenance or loss of the parasite.

210 What is of greater interest here is the comparison of \mathcal{R}_0 values between the
 211 density-dependent and frequency-dependent models. For the density-dependent model,

$$\mathcal{R}_0^{\text{DD}} = \frac{\left[b_{DD}^2 \cdot a_{MH}^{(2)} \cdot a_{HM} \cdot M^{(2)} \right] \cdot \left[c_{22}^2 \cdot H^{(2)} + c_{12}^2 \cdot H^{(1)} \right]}{\gamma \cdot \delta} \quad (\text{density dependent}). \quad (2)$$

210 Note that the mosquito biting rate term here has different units than in (1)—see Table
 211 1. Also note that there is no denominator term involving humans.

212 **Travel has different effects under frequency dependence versus
 213 density dependence**

214 There are obvious similarities in the \mathcal{R}_0 formulae, and we may compare them as follows:

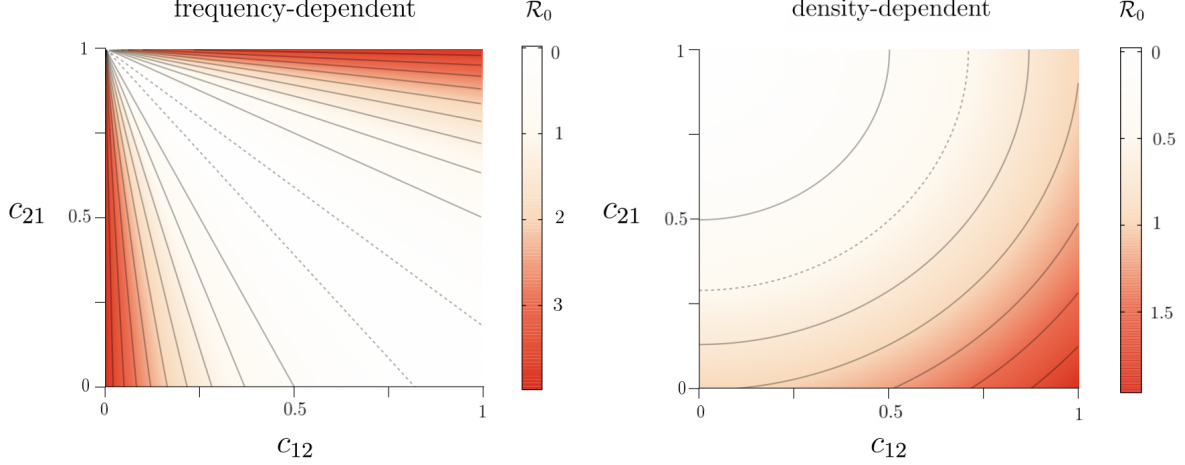


Figure 2: Contour plots of the basic reproduction number as a function of the visitation parameters (c_{12} and c_{21}) reveal a fundamentally different effect of human movement under frequency dependence (left) than under density dependence (right). In each panel, the dashed contour line represents $\mathcal{R}_0(c_{12}, c_{21}) = 1$, solid curves represent other values. These plots used a single set of parameters except for the c_{ij} , but plots using other values are similar, except the curvature (and steepness in the FD case) of the contour lines change when other parameters are varied. Values of the parameters used are $\gamma = 0.071$, $\lambda_1 = 50$, $\lambda_2 = 50$, $a_{MH}^{(1)} = 0$, $a_{HM}^{(2)} = 0.5$, $a_{HM}^{(1)} = 0.8$, $\delta = 0.02$, $b_{DD} = 0.000075$, and $b_{FD} = 0.0375$. The population sizes used are $H^{(1)} = H^{(2)} = 500$ and $M^{(2)} = 2500$. Calculations were done using expressions (1) and (2) for the basic reproduction numbers.

$$\mathcal{R}_0^{\text{FD}} = \mathcal{R}_0^{\text{DD}} \cdot \left(\frac{b_{FD}}{b_{DD}} \right)^2 \cdot \left[\frac{1}{(c_{22} \cdot H^{(2)} + c_{12} \cdot H^{(1)})} \right]^2 \quad (3)$$

215 The difference of greatest biological interest is in the rightmost term of (3) when
 216 considered along with (1) and (2). With increasing numbers of humans in patch 2
 217 (while maintaining constant mosquito density), the \mathcal{R}_0 for frequency dependence
 218 declines, whereas the \mathcal{R}_0 for density dependence increases. Note that increasing the
 219 number of humans in patch 2 can be accomplished either by increasing c_{22} or by
 220 increasing c_{12} . Increasing c_{22} increases spatial structure globally, whereas increasing c_{12}
 221 reduces spatial structure.

222 For the goal of parasite eradication, which in both models requires its eradication
 223 in patch 2, the contrast between the frequency- and density-dependent models is
 224 extreme when considering spatial structure of humans. Reducing travel out of patch 2
 225 increases \mathcal{R}_0 in the density-dependent case but decreases \mathcal{R}_0 in the
 226 frequency-dependent case. The converse is true of travel into patch 2 (c_{12}). Thus not
 227 only do the frequency-dependent and density-dependent models differ in the effect of
 228 changes in effective patch size (number of humans), but the effect of changing spatial
 229 structure differs between the models depending on whether travel involves humans

Notation	Description	Units
$H^{(k)}$	number of humans in patch k	individuals
$M^{(k)}$	number of mosquitoes in patch k	individuals
γ	recovery rate of infected humans	day $^{-1}$
b_{DD}	density-dependent biting rate	individual $^{-1}$ day $^{-1}$
b_{FD}	frequency-dependent biting rate	day $^{-1}$
δ	mosquito death rate	day $^{-1}$
c_{kj}	fraction of time patch k humans spend in patch j	dimensionless
a_{HM}	human to mosquito transmission probability	dimensionless
$a_{MH}^{(k)}$	patch k mosquito to human transmission probability	dimensionless

Table 1: Description of state variables and parameters in the mathematical models.

230 leaving patch 2 or coming into it.

231 Discussion

232 Our study is motivated by new technologies that are being used or will likely be used as
 233 interventions against vectored infectious diseases. They involve genetically modifying
 234 the vector to block its competence for parasite reproduction or transmission. As it is
 235 unlikely that any such interventions will cover entire vector populations, our interest lies
 236 in the consequences of unprotected vectors. In the absence of spatial structure, the
 237 overwhelming abundance of modified vectors would suppress the parasite, but with
 238 strong spatial structure, unprotected pockets/patches of vectors will enable the parasite
 239 to persist. What, then, is the effect of limited disruption of that spatial structure, as in
 240 the form of human travel?

241 We studied two types of well-established mathematical models of host-vector
 242 parasite dynamics. One model is a form of the long-used Ross-Macdonald model (e.g.,
 243 McCallum et al., 2001; Keeling and Rohani, 2008; Prosper et al., 2012; Ruktanonchai
 244 et al., 2016; Soriano-Paños et al., 2020), a model that assumes frequency-dependent
 245 behavior of mosquito biting. Frequency dependence is characterized by individual
 246 mosquitoes biting at a fixed rate, less per person as the local human population
 247 increases. The other model used here is similar except in assuming density-dependent
 248 biting rates; here individual humans are bitten at the same rate per mosquito regardless
 249 of how many people there are. All models assumed 2 patches of humans and their
 250 resident mosquitoes; the mosquitoes in one patch were blocked from transmission, but
 251 the mosquitoes in the other patch were fully competent. With strict spatial structure
 252 (no human movement), the parasite would be completely absent in one patch but
 253 present at high levels in the other patch.

254 From a casual consideration of previous work (e.g., Prosper et al., 2012; Bull
255 et al., 2019), we expected that any relaxation of spatial structure would reduce the
256 disease \mathcal{R}_0 if the disease-free patch was large enough relative to the diseased patch.
257 Thus sufficient human movement between the patches would eventually cause parasite
258 extinction. The results were unexpected in that (i) different directions of movement
259 (travel into or out of the patch) had opposing effects in a model, and (ii) those opposing
260 effects were reversed between the two types of model. In hindsight, differences between
261 the two models are understandable by considering the effect of increasing human
262 density in a patch. In the density-dependent model, an increase in humans in a patch
263 results in more mosquito biting (per mosquito); in the frequency-dependent model,
264 mosquitoes do not increase biting activity and added humans results in a ‘swamping’
265 effect where most humans are protected due to the presence of other humans. These
266 contrasting effects are at least broadly compatible with prior analyses that discovered
267 opposing effects of movement on \mathcal{R}_0 between frequency-dependent and
268 density-dependent assumptions in single-population models (Wonham et al., 2006).

269 An obvious next step is to understand mosquito biting dynamics as it bears on
270 disease transmission and human population structure. Simple extensions of
271 frequency-dependent and density-dependent models may accommodate both behaviors
272 as extremes in different biological realms, with high mosquito densities relative to
273 humans tending toward density dependence, low densities tending toward frequency
274 dependence (Gandon, 2018). However, additional complexities are possible: density and
275 frequency dependence may differentially accrue to humans and vectors, and indeed,
276 those two processes are not the only possible options for transmission dynamics
277 (McCallum et al., 2001; Wonham et al., 2006).

278 Joint spatial structure of both vectors and humans is likely to present a major
279 challenge to disease eradication by genetic modification of vector populations. Even
280 with seemingly perfect blocking by the genetic engineering in those populations where it
281 is implemented, potentially small unaltered vector populations will allow parasite
282 maintenance provided the humans remain appropriately structured. Such pockets of
283 escape may eventually be targeted for secondary interventions, but a major worry is
284 that small pockets of persistence will become foci for evolution of resistant parasites
285 that can then invade areas of more complete coverage. Understanding key dynamical
286 properties of real systems may help predict which types of interventions can be
287 combined to achieve local eradication.

288 Appendix

289 Two formulations of 2-patch vector-human models with 290 cross-patch visits by humans: density-dependent vs. 291 frequency-dependent transmission

292 Our models, written as systems of ordinary differential equations, track densities of
293 susceptible and infected humans and mosquitoes in two patches connected by human
294 movement. We let $H_s^{(k)}$ and $H_i^{(k)}$ be the densities of susceptible and infected human
295 hosts in patch $k \in \{1, 2\}$ and $M_s^{(k)}$ and $M_i^{(k)}$ be the densities of susceptible and infected
296 mosquitoes in patch k . The difference between the density-dependent and
297 frequency-dependent models is encapsulated in the mosquito “biting rates”. For the
298 density-dependent model, b_{DD} denotes the rate of biting per human per day by a given
299 mosquito. In the frequency-dependent model, b_{FD}/H denotes the rate of biting per
300 human per day by a given mosquito when the (local) density of humans is H . In other
301 words, a given mosquito doles out $b_{DD}H$ bites per day in the density-dependent model,
302 and b_{FD} bites per day in the frequency-dependent model. (When the number of humans
303 increases, density-dependent mosquitoes work harder; frequency-dependent mosquitoes
304 do not change their biting rate, but must allocate their bites among more humans.)

305 The probability that an uninfected human becomes infected when bitten by an
306 infected mosquito from patch k is given by $a_{MH}^{(k)}$. Dependence on the patch of the
307 infecting mosquito reflects the assumptions that the level of parasite suppression is
308 patch-dependent (as when the intervention is present in one patch but not the other)
309 and an absence of mosquito movement among patches. Human-to-mosquito
310 transmission is characterized by the parameter a_{HM} , which denotes the probability that
311 an uninfected mosquito becomes infected when it bites an infected human from either
312 patch; there is no patch-specific interference of human-to-mosquito transmission. Said
313 differently, patch-specific heterogeneity in transmission probability (and thus
314 transmission rate) of the disease from mosquitoes to humans is what characterizes the
315 effectiveness of the genetic intervention. Owing to the focus of intervention efforts on
316 the transmission from vector to human host, there is no such need to introduce
317 patch-specific differences in human-to-mosquito transmission.

318 Let δ denote the death rate of mosquitoes and γ the recovery rate of an infected
319 human. We also let λ_k be the birth rate of susceptible mosquitoes in patch k . The
320 equilibrium density of mosquitoes in patch k is, thus, given by λ_k/δ . We focus on
321 parasite transmission dynamics when mosquito density is constant. The fraction of time
322 a human residing in patch 1 spends in patch 1 (resp., patch 2) is denoted by c_{11} (resp.,
323 c_{12}), where $c_{11} + c_{12} = 1$. Similarly, human residents of patch 2 spend fractions c_{21} and

³²⁴ c_{22} in patches 1 and 2. Note that our human movement model is one of “visitation”
³²⁵ rather than actual migration. An example would be people who commute between their
³²⁶ home city and another for work. We assume that $0 \leq c_{12} < 1$ and $0 \leq c_{21} < 1$ to ensure
³²⁷ that there are actually people in each patch.

³²⁸ **Density-dependent transmission**

³²⁹ In the case of density-dependent transmission, infection rates for mosquitoes and
³³⁰ humans have a mass-action dependence on mosquito and human densities.

$$\begin{aligned}\dot{H}_s^{(1)} &= -b_{DD}H_s^{(1)} \left[c_{11}a_{MH}^{(1)}M_i^{(1)} + c_{12}a_{MH}^{(2)}M_i^{(2)} \right] + \gamma H_i^{(1)} \\ \dot{H}_i^{(1)} &= b_{DD}H_s^{(1)} \left[c_{11}a_{MH}^{(1)}M_i^{(1)} + c_{12}a_{MH}^{(2)}M_i^{(2)} \right] - \gamma H_i^{(1)} \\ \dot{M}_s^{(1)} &= \lambda_1 - b_{DD}a_{HM}M_s^{(1)} \left[c_{11}H_i^{(1)} + c_{21}H_i^{(2)} \right] - \delta M_s^{(1)} \\ \dot{M}_i^{(1)} &= b_{DD}a_{HM}M_s^{(1)} \left[c_{11}H_i^{(1)} + c_{21}H_i^{(2)} \right] - \delta M_i^{(1)} \\ \\ \dot{H}_s^{(2)} &= -b_{DD}H_s^{(2)} \left[c_{21}a_{MH}^{(1)}M_i^{(1)} + c_{22}a_{MH}^{(2)}M_i^{(2)} \right] + \gamma H_i^{(2)} \\ \dot{H}_i^{(2)} &= b_{DD}H_s^{(2)} \left[c_{21}a_{MH}^{(1)}M_i^{(1)} + c_{22}a_{MH}^{(2)}M_i^{(2)} \right] - \gamma H_i^{(2)} \\ \dot{M}_s^{(2)} &= \lambda_2 - b_{DD}a_{HM}M_s^{(2)} \left[c_{22}H_i^{(2)} + c_{12}H_i^{(1)} \right] - \delta M_s^{(2)} \\ \dot{M}_i^{(2)} &= b_{DD}a_{HM}M_s^{(2)} \left[c_{22}H_i^{(2)} + c_{12}H_i^{(1)} \right] - \delta M_i^{(2)}\end{aligned}$$

³³¹ **Frequency-dependent transmission**

³³² Let $H^{(k)} = H_s^{(k)} + H_i^{(k)}$ denote the total number of humans who reside in patch k .
³³³ Then, for example, mosquitoes residing in patch 1 will see a mix of humans: $c_{11}H^{(1)}$
³³⁴ residents of patch 1 who are not visiting patch 2, and $c_{21}H^{(2)}$ residents of patch 2 who
³³⁵ are visiting patch 1. The ‘effective’ number of humans in patch 1 (i.e., the number of
³³⁶ humans experienced by mosquitoes in patch 1) is thus $\tilde{H}^{(1)} \equiv c_{11}H^{(1)} + c_{21}H^{(2)}$.
³³⁷ Similarly, the effective number of humans in patch 2 is $\tilde{H}^{(2)} \equiv c_{12}H^{(1)} + c_{22}H^{(2)}$. In the
³³⁸ frequency-dependent transmission framework, a mosquito’s bites are randomly allocated
³³⁹ to this mix of humans.

$$\begin{aligned}
\dot{H}_s^{(1)} &= -b_{FD} H_s^{(1)} \left[\frac{c_{11} a_{MH}^{(1)} M_i^{(1)}}{\tilde{H}^{(1)}} + \frac{c_{12} a_{MH}^{(2)} M_i^{(2)}}{\tilde{H}^{(2)}} \right] + \gamma H_i^{(1)} \\
\dot{H}_i^{(1)} &= b_{FD} H_s^{(1)} \left[\frac{c_{11} a_{MH}^{(1)} M_i^{(1)}}{\tilde{H}^{(1)}} + \frac{c_{12} a_{MH}^{(2)} M_i^{(2)}}{\tilde{H}^{(2)}} \right] - \gamma H_i^{(1)} \\
\dot{M}_s^{(1)} &= \lambda_1 - b_{FD} a_{HM} M_s^{(1)} \cdot \left[\frac{c_{11} H_i^{(1)} + c_{21} H_i^{(2)}}{\tilde{H}^{(1)}} \right] - \delta M_s^{(1)} \\
\dot{M}_i^{(1)} &= b_{FD} a_{HM} M_s^{(1)} \cdot \left[\frac{c_{11} H_i^{(1)} + c_{21} H_i^{(2)}}{\tilde{H}^{(1)}} \right] - \delta M_i^{(1)} \\
\\
\dot{H}_s^{(2)} &= -b_{FD} H_s^{(2)} \left[\frac{c_{22} a_{MH}^{(2)} M_i^{(2)}}{\tilde{H}^{(2)}} + \frac{c_{21} a_{MH}^{(1)} M_i^{(1)}}{\tilde{H}^{(1)}} \right] + \gamma H_i^{(2)} \\
\dot{H}_i^{(2)} &= b_{FD} H_s^{(2)} \left[\frac{c_{22} a_{MH}^{(2)} M_i^{(2)}}{\tilde{H}^{(2)}} + \frac{c_{21} a_{MH}^{(1)} M_i^{(1)}}{\tilde{H}^{(1)}} \right] - \gamma H_i^{(2)} \\
\dot{M}_s^{(2)} &= \lambda_2 - b_{FD} a_{HM} M_s^{(2)} \left[\frac{c_{22} H_i^{(2)} + c_{12} H_i^{(1)}}{\tilde{H}^{(2)}} \right] - \delta M_s^{(2)} \\
\dot{M}_i^{(2)} &= b_{FD} a_{HM} M_s^{(2)} \left[\frac{c_{22} H_i^{(2)} + c_{12} H_i^{(1)}}{\tilde{H}^{(2)}} \right] - \delta M_i^{(2)}
\end{aligned}$$

340 Density-dependent \mathcal{R}_0 calculations

341 The basic reproduction number, especially for vectored disease models like those we
 342 consider, can be defined in several ways. These definitions give the same threshold
 343 condition ($\mathcal{R}_0 < 1$) for the stability of the disease-free steady-state. Due to the
 344 multiphasic nature of vectored disease transmission, differences between definitions of
 345 the basic reproduction number for diseases like malaria can often be reconciled by
 346 realizing, say, one is the square of the other. A more fundamental issue in defining \mathcal{R}_0
 347 for mosquito-borne disease is the complexity that arises from having both human and
 348 vectors host the disease agent. Is \mathcal{R}_0 the number of secondary mosquito infections due
 349 to a small number of primarily infected mosquitoes in an otherwise susceptible
 350 population, or the number of secondary human infections due to a small number of
 351 initially infected humans, or some combination of the two? While the fates of
 352 mosquitoes and humans over the course of an epidemic are coupled, the mosquito- and
 353 human-centric basic reproduction numbers are indeed distinct quantities, agreeing only
 354 if the disease persists in the population at equilibrium.

355 To calculate the basic reproduction number \mathcal{R}_0 for the pathogen in mosquitoes, we
 356 assume that there is a small density of (primary) infected mosquitoes, $M_i^{(1)}(0), M_i^{(2)}(0)$,
 357 in patches 1 and 2, respectively, and no infected humans. In this initial phase, the
 358 density of susceptible mosquitoes is approximately $M^{(1)}$ in patch 1 and $M^{(2)}$ in patch 2,
 359 while the numbers of susceptible humans is $H^{(1)}$ in patch 1 and $H^{(2)}$ in patch 2. To
 360 compute the numbers of secondary infections of mosquitoes in each patch, we must
 361 consider two steps: mosquito-to-human followed by human-to-mosquito transmission.

362 1. The number of humans directly infected from primary mosquitoes before they die
 363 is:

- in patch 1:

$$H_{i,\text{new}}^{(1)} = \frac{b_{DD} H^{(1)}}{\delta} \cdot \left[c_{11} a_{MH}^{(1)} \cdot M_i^{(1)}(0) + c_{12} a_{MH}^{(2)} \cdot M_i^{(2)}(0) \right]$$

- in patch 2:

$$H_{i,\text{new}}^{(2)} = \frac{b_{DD} H^{(2)}}{\delta} \cdot \left[c_{21} a_{MH}^{(1)} \cdot M_i^{(1)}(0) + c_{22} a_{MH}^{(2)} \cdot M_i^{(2)}(0) \right]$$

364 2. The number of mosquitoes infected by these newly infected humans before they
 365 recover is:

- in patch 1:

$$M_{i,\text{new}}^{(1)} = \frac{b_{DD} a_{HM} M^{(1)}}{\gamma} \cdot \left[c_{11} H_{i,\text{new}}^{(1)} + c_{21} H_{i,\text{new}}^{(2)} \right]$$

- in patch 2:

$$M_{i,\text{new}}^{(2)} = \frac{b_{DD} a_{HM} M^{(2)}}{\gamma} \cdot \left[c_{12} H_{i,\text{new}}^{(1)} + c_{22} H_{i,\text{new}}^{(2)} \right]$$

366 Note that mosquito death rate δ corresponds to mean lifetime $1/\delta$; similarly, $1/\gamma$
 367 corresponds to the mean time before an infected human recovers. Combining the above
 368 two steps allows us to specify patterns of secondary infection (per primary infected
 369 mosquito in each patch) in the matrix

$$R = \begin{bmatrix} R(1,1) & R(1,2) \\ R(2,1) & R(2,2) \end{bmatrix},$$

370 where $R(j, k)$ denotes the number of secondary mosquito infections in patch j that

371 arose from primarily infected mosquitoes in patch k , for $j, k \in \{1, 2\}$. Consequently, the
 372 j th row sum gives the number of secondary mosquito infections in patch j , and the k th
 373 column sum is the total number of secondary infections due to initially infected
 374 mosquitoes in patch k . Tracking the patterns of infection in both patches, we find that

$$R(1, 1) = \frac{b_{DD}^2 \cdot a_{HM} \cdot M^{(1)} \cdot a_{MH}^{(1)}}{\gamma \cdot \delta} \cdot \left[c_{11}^2 \cdot H^{(1)} + c_{21}^2 \cdot H^{(2)} \right],$$

$$R(1, 2) = \frac{b_{DD}^2 \cdot a_{HM} \cdot M^{(1)} \cdot a_{MH}^{(2)}}{\gamma \cdot \delta} \cdot \left[c_{12} \cdot c_{11} \cdot H^{(1)} + c_{21} \cdot c_{22} \cdot H^{(2)} \right],$$

$$R(2, 1) = \frac{b_{DD}^2 \cdot a_{HM} \cdot M^{(2)} \cdot a_{MH}^{(1)}}{\gamma \cdot \delta} \cdot \left[c_{21} \cdot c_{22} \cdot H^{(2)} + c_{12} \cdot c_{11} \cdot H^{(1)} \right],$$

$$R(2, 2) = \frac{b_{DD}^2 \cdot a_{HM} \cdot M^{(2)} \cdot a_{MH}^{(2)}}{\gamma \cdot \delta} \cdot \left[c_{22}^2 \cdot H^{(2)} + c_{12}^2 \cdot H^{(1)} \right].$$

375 Note that each of the four secondary transmission terms above has two components:
 376 one corresponding to a susceptible human from patch 1 being infected by a primary
 377 infected mosquito from the designated patch, and one corresponding to a susceptible
 378 human from patch 2 being infected by a primary infected mosquito. Recall that
 379 mosquitoes are tied to their patch; only humans visit the other patch. For example,
 380 $R(1, 2)$ records the number of secondary infections of mosquitoes living in patch 1 that
 381 arose from a primary infected mosquito in patch 2. There are two patterns of human
 382 visitation that can lead to this event. (1) encoded in the term $c_{12}c_{11}H^{(1)}$ on the
 383 right-hand side of the $R(1, 2)$ expression: in the first phase, a human in patch 1 visits
 384 patch 2 and is infected by a primary mosquito there (and the human returns to its
 385 home patch); in the second phase, the newly infected human stays in patch 1 and
 386 infects a susceptible mosquito there. (2) encoded in the term $c_{22}c_{21}H^{(2)}$ on the
 387 right-hand side of the $R(1, 2)$ expression: in the first phase, a human in patch 2 remains
 388 in patch 2 and is infected by a primary mosquito there; in the second phase, the newly
 389 infected human visits patch 1 and infects a susceptible mosquito there.

390 The *basic reproduction number* $\mathcal{R}_0^{\text{DD}}$ for the density-dependent transmission model
 391 is the leading eigenvalue of the matrix R . The special case of no mosquito-to-human
 392 transmission in patch 1 (i.e., $a_{MH}^{(1)} = 0$) is interesting in that $R(1, 1) = 0 = R(2, 1)$ and
 393 hence $\mathcal{R}_0^{\text{DD}} = R(2, 2)$.

394 Frequency-dependent \mathcal{R}_0 calculations

395 Similar to the above case, the calculation of a mosquito-centric \mathcal{R}_0 for the
 396 frequency-dependent case begins with an assumption that there is a small density of
 397 (primary) infected mosquitoes, $M_i^{(1)}(0), M_i^{(2)}(0)$, in patches 1 and 2, respectively, and

398 no infected humans. In this initial phase, the density of susceptible mosquitoes is
 399 approximately $M^{(1)}$ in patch 1 and $M^{(2)}$ in patch 2, while the numbers of susceptible
 400 humans is $H^{(1)}$ in patch 1 and $H^{(2)}$ in patch 2. To compute the numbers of secondary
 401 infections of mosquitoes in each patch, we must consider two steps: mosquito-to-human
 402 followed by human-to-mosquito transmission.

403 1. The number of humans directly infected from primary mosquito before it dies is:

- in patch 1:

$$H_{i,\text{new}}^{(1)} = \frac{b_{FD} H^{(1)}}{\delta} \cdot \left[\frac{c_{11} a_{MH}^{(1)}}{\tilde{H}^{(1)}} \cdot M_i^{(1)}(0) + \frac{c_{12} a_{MH}^{(2)}}{\tilde{H}^{(2)}} \cdot M_i^{(2)}(0) \right]$$

- in patch 2:

$$H_{i,\text{new}}^{(2)} = \frac{b_{FD} H^{(2)}}{\delta} \cdot \left[\frac{c_{21} a_{MH}^{(1)}}{\tilde{H}^{(1)}} \cdot M_i^{(1)}(0) + \frac{c_{22} a_{MH}^{(2)}}{\tilde{H}^{(2)}} \cdot M_i^{(2)}(0) \right]$$

404 2. The number of mosquitoes infected by these newly infected humans before they
 405 recover is:

- in patch 1:

$$M_{i,\text{new}}^{(1)} = \frac{b_{FD} a_{HM} M^{(1)}}{\gamma} \cdot \frac{c_{11} H_{i,\text{new}}^{(1)} + c_{21} H_{i,\text{new}}^{(2)}}{\tilde{H}^{(1)}}$$

- in patch 2:

$$M_{i,\text{new}}^{(2)} = \frac{b_{FD} a_{HM} M^{(2)}}{\gamma} \cdot \frac{c_{12} H_{i,\text{new}}^{(1)} + c_{22} H_{i,\text{new}}^{(2)}}{\tilde{H}^{(2)}}$$

406 Putting these together allows us to specify patterns of secondary infection (per
 407 primary infected mosquito in each patch) in the matrix

$$R' = \begin{bmatrix} R'(1,1) & R'(1,2) \\ R'(2,1) & R'(2,2) \end{bmatrix},$$

408 where $R(j, k)$ denotes the number of secondary mosquito infections in patch j that
 409 arose from primary infected mosquitoes in patch k , for $j, k \in \{1, 2\}$. Tracking the
 410 patterns of infection in both patches, we arrive at

$$R'(1,1) = \frac{b_{FD}^2 \cdot a_{HM} \cdot a_{MH}^{(1)} \cdot M^{(1)} \cdot [c_{11}^2 \cdot H^{(1)} + c_{21}^2 \cdot H^{(2)}]}{\delta \cdot \gamma \cdot [\tilde{H}^{(1)}]^2},$$

$$R'(1,2) = \frac{b_{FD}^2 \cdot a_{HM} \cdot a_{MH}^{(2)} \cdot M^{(1)} \cdot [c_{12} \cdot c_{11} \cdot H^{(1)} + c_{22} \cdot c_{21} \cdot H^{(2)}]}{\delta \cdot \gamma \cdot \tilde{H}^{(1)} \cdot \tilde{H}^{(2)}},$$

$$R'(2,1) = \frac{b_{FD}^2 \cdot a_{HM} \cdot a_{MH}^{(1)} \cdot M^{(2)} \cdot [c_{21} \cdot c_{22} \cdot H^{(2)} + c_{11} \cdot c_{12} \cdot H^{(1)}]}{\delta \cdot \gamma \cdot \tilde{H}^{(1)} \cdot \tilde{H}^{(2)}},$$

$$R'(2,2) = \frac{b_{FD}^2 \cdot a_{HM} \cdot a_{MH}^{(2)} \cdot M^{(2)} \cdot [c_{22}^2 \cdot H^{(2)} + c_{12}^2 \cdot H^{(1)}]}{\delta \cdot \gamma \cdot [\tilde{H}^{(2)}]^2}.$$

411 The *basic reproduction number* $\mathcal{R}_0^{\text{FD}}$ for the frequency-dependent transmission model is
 412 the leading eigenvalue of the matrix R' . As in the density-dependent transmission
 413 model, the special case of no mosquito-to-human transmission in patch 1 (i.e., $a_{MH}^{(1)} = 0$)
 414 results in $R'(1,1) = 0 = R'(2,1)$ and hence $\mathcal{R}_0^{\text{FD}} = R'(2,2)$. If we assume both $a_{MH}^{(1)} = 0$
 415 and $c_{12} = 0$, then we obtain a stark difference between these models:

416 $\mathcal{R}_0^{\text{DD}} = \frac{b_{DD}^2 a_{MH}^{(2)} a_{HM} M^{(1)}}{\delta \gamma} c_{22}^2 H^{(2)}$ for the density-dependent model, and

417 $\mathcal{R}_0^{\text{FD}} = \frac{b_{FD}^2 a_{MH}^{(2)} a_{HM} M^{(2)}}{\delta \gamma H^{(2)}}$ for the frequency-dependent model. Thus, one-way visitation to
 418 a patch with perfect cargo has a strong effect in the density-dependent model, but no
 419 effect in the frequency-dependent model. In fact, the latter $\mathcal{R}_0^{\text{FD}}$ is in the standard form
 420 for a Ross-Macdonald model with no patch structure.

421 Notice that mosquito and human densities in the terms characterizing the basic
 422 reproduction number in the frequency-dependent model appear in ratio form M/H ,
 423 while in the density-dependent model they appear in product form MH .

424 Our \mathcal{R}_0 calculations, for both density- and frequency-dependent transmission,
 425 were based on computing numbers of secondarily infected mosquitoes that arose from
 426 the primary mosquito infections. Since human and mosquito infections are intertwined
 427 due to the nature of vector transmission, it should not be surprising that the threshold
 428 $\mathcal{R}_0 = 1$ above which human infection persists is the same as the one that guarantees
 429 persistence of mosquito infection. In numerical solutions of our differential equations
 430 (not shown), we saw positive equilibrium densities of both infected mosquitoes and
 431 infected humans precisely when $\mathcal{R}_0 > 1$.

432 References

433 Anzo-Hernández, A., Bonilla-Capilla, B., Velázquez-Castro, J., Soto-Bajo, M., and
 434 Fraguella-Collar, A. The risk matrix of vector-borne diseases in metapopulation
 435 networks and its relation with local and global R_0 . *Communications in Nonlinear*

436 *Science and Numerical Simulation*, Mar. 2019, **68**:1–14. ISSN 1007-5704. doi:
437 10.1016/j.cnsns.2018.06.006. URL
438 <http://www.sciencedirect.com/science/article/pii/S1007570418301837>.

439 Bull, J. J., Remien, C. H., and Krone, S. M. Gene-drive-mediated extinction is
440 thwarted by population structure and evolution of sib mating. *Evolution, Medicine,*
441 *and Public Health*, 2019, **2019**(1):66–81. ISSN 2050-6201. doi: 10.1093/emph/eoz014.

442 Burt, A. Heritable strategies for controlling insect vectors of disease. *Philosophical*
443 *Transactions of the Royal Society of London. Series B, Biological Sciences*, 2014, **369**
444 (1645):20130432. ISSN 1471-2970. doi: 10.1098/rstb.2013.0432.

445 Cosner, C., Beier, J. C., Cantrell, R. S., Impoinvil, D., Kapitanski, L., Potts, M. D.,
446 Troyo, A., and Ruan, S. The effects of human movement on the persistence of
447 vector-borne diseases. *Journal of Theoretical Biology*, June 2009, **258**(4):550–560.
448 ISSN 1095-8541. doi: 10.1016/j.jtbi.2009.02.016.

449 Evans, B. R., Kotsakiozi, P., Costa-da Silva, A. L., Ioshino, R. S., Garziera, L., Pedrosa,
450 M. C., Malavasi, A., Virginio, J. F., Capurro, M. L., and Powell, J. R. Transgenic
451 Aedes aegypti mosquitoes transfer genes into a natural population. *Scientific Reports*,
452 2019, **9**(1):13047. ISSN 2045-2322. doi: 10.1038/s41598-019-49660-6.

453 Gandon, S. Evolution and manipulation of vector host choice. *The American*
454 *Naturalist*, 2018, **192**(1):23–34. ISSN 1537-5323. doi: 10.1086/697575.

455 Gantz, V. M., Jasinskiene, N., Tatarenkova, O., Fazekas, A., Macias, V. M., Bier, E.,
456 and James, A. A. Highly efficient Cas9-mediated gene drive for population
457 modification of the malaria vector mosquito *Anopheles stephensi*. *Proceedings of the*
458 *National Academy of Sciences of the United States of America*, Dec. 2015, **112**(49):
459 E6736–6743. ISSN 1091-6490. doi: 10.1073/pnas.1521077112.

460 Gould, F. Broadening the application of evolutionarily based genetic pest management.
461 *Evolution*, 2008, **62**(2):500–510. ISSN 0014-3820. doi:
462 10.1111/j.1558-5646.2007.00298.x.

463 Gould, F., Magori, K., and Huang, Y. Genetic strategies for controlling mosquito-borne
464 diseases. *American Scientist*, 2006, **94**:238 – 346.

465 Hoffmann, A. A., Montgomery, B. L., Popovici, J., Iturbe-Ormaetxe, I., Johnson, P. H.,
466 Muzzi, F., Greenfield, M., Durkan, M., Leong, Y. S., Dong, Y., Cook, H., Axford, J.,
467 Callahan, A. G., Kenny, N., Omodei, C., McGraw, E. A., Ryan, P. A., Ritchie, S. A.,
468 Turelli, M., and O'Neill, S. L. Successful establishment of Wolbachia in Aedes
469 populations to suppress dengue transmission. *Nature*, Aug. 2011, **476**(7361):454–457.
470 ISSN 1476-4687. doi: 10.1038/nature10356.

471 Keeling, M. J. and Rohani, P. *Modeling Infectious Diseases in Humans and Animals*.
472 Princeton University Press, 2008. ISBN 978-0-691-11617-4. Google-Books-ID:
473 G8enmS23c6YC.

474 Khamis, D., El Mouden, C., Kura, K., and Bonsall, M. B. The effect of dispersal and
475 preferential mating on the genetic control of mosquitoes. preprint, Ecology, May
476 2020. URL <http://biorxiv.org/lookup/doi/10.1101/2020.05.25.114413>.

477 McCallum, H., Barlow, N., and Hone, J. How should pathogen transmission be
478 modelled? *Trends in Ecology & Evolution*, June 2001, **16**(6):295–300. ISSN
479 1872-8383. doi: 10.1016/s0169-5347(01)02144-9.

480 North, A., Burt, A., Godfray, H. C. J., and Buckley, Y. Modelling the spatial spread of
481 a homing endonuclease gene in a mosquito population. *The Journal of Applied
482 Ecology*, Oct. 2013, **50**(5):1216–1225. ISSN 0021-8901. doi: 10.1111/1365-2664.12133.

483 North, A. R., Burt, A., and Godfray, H. C. J. Modelling the potential of genetic control
484 of malaria mosquitoes at national scale. *BMC Biology*, 2019, **17**(1):26. ISSN
485 1741-7007. doi: 10.1186/s12915-019-0645-5.

486 Prosper, O., Ruktanonchai, N., and Martcheva, M. Assessing the role of spatial
487 heterogeneity and human movement in malaria dynamics and control. *Journal of
488 Theoretical Biology*, June 2012, **303**:1–14. ISSN 1095-8541. doi:
489 10.1016/j.jtbi.2012.02.010.

490 Ruktanonchai, N. W., Smith, D. L., and De Leenheer, P. Parasite sources and sinks in a
491 patched Ross-Macdonald malaria model with human and mosquito movement:
492 Implications for control. *Mathematical Biosciences*, 2016, **279**:90–101. ISSN
493 1879-3134. doi: 10.1016/j.mbs.2016.06.012.

494 Schmidt, T. L., Barton, N. H., Rašić, G., Turley, A. P., Montgomery, B. L.,
495 Iturbe-Ormaetxe, I., Cook, P. E., Ryan, P. A., Ritchie, S. A., Hoffmann, A. A.,
496 O'Neill, S. L., and Turelli, M. Local introduction and heterogeneous spatial spread of
497 dengue-suppressing Wolbachia through an urban population of Aedes aegypti. *PLoS
498 Biology*, 2017, **15**(5):e2001894. ISSN 1545-7885. doi: 10.1371/journal.pbio.2001894.

499 Soriano-Paños, D., Arias-Castro, J. H., Reyna-Lara, A., Martínez, H. J., Meloni, S., and
500 Gómez-Gardeñes, J. Vector-borne epidemics driven by human mobility. *Physical
501 Review Research*, Mar. 2020, **2**(1):013312. ISSN 2643-1564. doi:
502 10.1103/PhysRevResearch.2.013312. URL
503 <https://link.aps.org/doi/10.1103/PhysRevResearch.2.013312>.

504 Wonham, M. J., Lewis, M. A., Rencławowicz, J., and van den Driessche, P.
505 Transmission assumptions generate conflicting predictions in host-vector disease
506 models: a case study in West Nile virus. *Ecology Letters*, June 2006, **9**(6):706–725.
507 ISSN 1461-0248. doi: 10.1111/j.1461-0248.2006.00912.x.

508 Xue, L., Fang, X., and Hyman, J. M. Comparing the effectiveness of different strains of
509 Wolbachia for controlling chikungunya, dengue fever, and zika. *PLoS Neglected
510 Tropical Diseases*, 2018, **12**(7):e0006666. ISSN 1935-2735. doi:
511 10.1371/journal.pntd.0006666.